



Synthesis of TS-1 on porous glass beads for catalytic oxidative desulfurization



C. Shen, Y.J. Wang^{*}, J.H. Xu, G.S. Luo^{*}

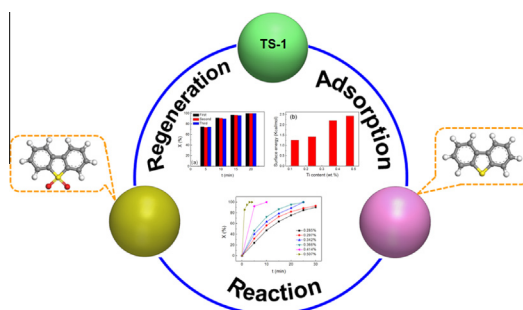
State Key Laboratory of Chemical Engineering, Department of Chemical Engineering, Tsinghua University, Beijing 100084, China

HIGHLIGHTS

- TS-1 particles on porous glass have been prepared and used for ODS.
- Complete conversion of DBT was reached within 3 min.
- The catalytic activity was dominated by coordinated state of titanium species.

GRAPHICAL ABSTRACT

Porous glass beads supported with TS-1 particles have been successfully prepared and used as the catalyst for oxidative desulfurization of dibenzothiophene (DBT) and 4,6-dimethyldibenzothiophene (4,6-DMDBT). The composite material showed high catalytic activity and good stability. The coordinated state of titanium species plays a key role in catalytic activity.



ARTICLE INFO

Article history:

Received 10 May 2014

Received in revised form 7 August 2014

Accepted 9 August 2014

Available online 19 August 2014

Keywords:

Supported TS-1

Oxidative desulfurization

Catalytic performance

ABSTRACT

Porous glass supported with titanium silicalite (TS-1) particles were successfully prepared and used for oxidative desulfurization (ODS) of dibenzothiophene (DBT) and 4,6-dimethyldibenzothiophene (4,6-DMDBT). Uniform-sized TS-1 particles were homogeneously dispersed on the surface of the porous glass beads. Effects of reaction duration, catalyst content, initial concentration, oxidant amount, and temperature on conversions were investigated. The prepared catalysts showed excellent catalytic performance. The optimal mole ratio of oxidant-to-DBT was 10 or 15. Complete conversion was obtained within 3 min at 343 K using catalyst with Ti content of 0.507 wt.%. Compared with other studies, the space-time yield was increased by one order of magnitude without any addition of solvent or metal nanoparticles. Experimental results and computer simulations revealed that the coordinated state of Ti species has a key role in the catalytic activity. Spent catalyst would be regenerated by heating at high temperature, no decrease was observed in catalytic activity after three cycles.

© 2014 Elsevier B.V. All rights reserved.

1. Introduction

Removal of organosulfur compounds contained in petroleum has received increasing attention in recent years. The combustion

of these sulfur-containing compounds leads to the formation of sulfur oxide which contributes to acid rain, depletion of the ozone layer, and smog generation. The US Environmental Protection Agency (EPA) has issued a sulfur standard of 15 ppm in diesel fuel in June 2006 [1,2]. China has implemented the Euro V (10 ppm) standard in Beijing in recent years. Thus, the production of ultra clean fuels has become an enormous challenge for current desulfurization methods.

^{*} Corresponding authors. Tel./fax: +86 010 62788568.

E-mail addresses: wangyujun@mail.tsinghua.edu.cn (Y.J. Wang), gsluo@tsinghua.edu.cn (G.S. Luo).

Hydrodesulfurization (HDS), the conventional method for reducing sulfur content in fuels, requires huge operating and capital costs in presence of some refractory sulfur compounds, such as DBT and its derivatives [3–6]. By contrast, ODS has been considered as one of the most promising alternatives for obtaining ultra-low sulfur fuels because of several attractive features, such as low operating temperature, mild pressure, and low cost of operation [7–10]. In addition, ODS has one significant advantage over HDS, i.e., DBT and its derivatives, which are the least reactive compounds in HDS, are highly reactive in ODS because of the high electron density on the sulfur atom.

Titanium silicalite (TS-1) is an important catalyst for selective oxidation of organic compounds. Several studies have recently been performed on the catalytic activity of TS-1 for organic sulfur compounds under mild conditions [11–28]. Thasaneeya et al. [21] used *n*-dodecane containing thiophene as a model feed for oxidative extraction, and TS-1 with large crystal size was used as the catalyst. Approximately 30% thiophene removal was obtained from 1000 ppm through homogeneous extraction after 5 h. Higher removal rates of 75% and 95% were reached using 1.0 and 1.8 g of TS-1 as the catalyst after 6 h, respectively. Moreover, the oxidation activity increased with the increase in solvent-to-oil ratio.

The function of TS-1 nanoparticles as the catalyst for ODS is limited by the long reaction time resulted from their low catalytic activity. Three solutions were proposed in recent years to solve this limitation. First is the addition of polar solvents, such as water or alcohol, similar to the experiment conducted by Thasaneeya et al. [21].

Another method is adding metal nanoparticles on TS-1 surfaces. Jose et al. [23] used TS-1 loaded with copper as the catalyst for ODS and reported that the conversion of thiophene increases gradually when the copper amount increases to 1.05%, however further increase in copper amount to 1.44% would lead to decrease in conversion of thiophene. Conversions for pure TS-1 and 1.05% copper-loaded TS-1 particles were 47% and 57%, respectively. Similar results have also been reported by Kong [14]. In gasoline model composed of thiophene in *n*-octane, the catalyst with Ag loading of 0.06 wt.% shows the highest activity with 95% conversion after 4 h.

The third method involves the preparation of mesoporous TS-1, which has been increasingly investigated. Zhu [29] reported that the tetrahedrally coordinated Ti species in the framework functions as the catalytic activity center during ODS process. To obtain more explored activity centers, mesoporous TS-1 zeolites have been synthesized using cetyl trimethyl ammonium bromide (CTAB) as the mesoporegen under the assistance of ethanol. The mesoporous TS-1 and TS-1 zeolite provided 75% and 50% of conversions, respectively, after 5 h using *t*-butanol as the solvent.

Thus, ODS using TS-1 as the catalyst still faces great challenges for industrialization because of the long reaction time, difficulty in catalyst separation, addition of polar solvent, such as alcohol, and addition of noble metal on the catalyst. Catalysts with high activity, easy recyclability, and low cost are still urgently needed.

In this study, we explored the feasibility of using TS-1 supported on porous glass as catalyst for ODS. To the best of our knowledge, application of immobilized TS-1 in ODS has not been reported yet. Fixing TS-1 nanoparticles on the surface of porous glass contributes to the easy separation from the reaction system and the large contact area with reactants by avoiding the agglomeration of TS-1 nanoparticles. Catalytic activity and stability are investigated for the removal of sulfur-containing compounds from liquid hydrocarbon solutions. The DBT solution dissolved in octane is used as the model fuel. Effects of reaction time, catalyst content, initial concentration, oxidant amount, and temperature have been studied systematically in relation to the change in the conversion. Regeneration performance was also investigated.

2. Experimental

2.1. Materials and chemicals

Soda-lime glass microbeads with diameters ranging from 75 to 150 μm and composed of 59.7 wt.% SiO_2 , 25.1 wt.% Na_2O , 9.8 wt.% MgO , and 4.9 wt.% CaO were obtained from Hebei Chiye Corporation. The beads were sieved before application, and beads with sizes ranging from 95 to 105 μm were taken as samples. Tetraethyl orthosilicate (TEOS), titanium ethoxide (TEOT), isopropanol and cumene hydroperoxide (CHP) were purchased from J&K Chemical Ltd. Tetrapropylammonium hydroxide (TPAOH) with a concentration of 1 M in water was from Aladdin Co., Ltd. Concentrated hydrochloric acid with a concentration of 36–38 wt.% and analytical grade octane was purchased from Fuchen Chemical Plant in Tianjin, China. DBT and 4,6-DMDBT were purchased from Acros Organics. All chemicals were used as received without further treatment.

2.2. Preparation and characteristic of porous glass beads supported with TS-1 particles

The porous glass beads were prepared by the subcritical water treatment method described in our previous study [25,26]. First, 200 g of water and 5 g of glass beads were placed in a tank reactor with a volume of 250 cm^3 . The reactor was then gradually heated to 573 ± 0.1 K, and the pressure was increased from atmospheric pressure to almost 8 MPa. The subcritical state was maintained for 60 min, and then the reactor was cooled naturally to room temperature. After filtration, the porous glass beads were treated by 0.5 M hydrochloric acid solution for 9 h in a shaking bath at a speed of 130 rpm at 303 K to remove the metal ions contained in the shell part of the porous glass beads. Afterward, the porous glass beads were washed several times with deionized water. The porous glass beads were calcined at 593 K for 2 h before further use.

The supported TS-1 particles on porous glass beads were prepared as follows: 3 mL of TPAOH and 0.25 mL of water were added to 4 mL of TEOS under constant stirring. The clear solution became cloudy, but became clear again after further stirring for 30 min. The solution containing 0.06 mL of TEOT and 3 mL of isopropanol was then added dropwise. Addition of isopropanol helps to slow down the hydrolysis rate of TEOT and better insertion of Ti element into the framework. Then the mixture was further stirred for 12 h and transferred to a water bath maintained at 353 K, and then stirred for 3 h to completely evaporate the alcohol. After a cooling-off period, 10 g of water and the prepared porous glass beads with the amount ranging from 1 to 6 g were added. The solid–liquid mixture was then transferred to a 50 mL Teflon-lined stainless-steel autoclave and crystallized for 48 h at 403 K. The obtained porous glass was washed several times by deionized water and calcined in air at 823 K for 6 h.

The morphology of the porous glass beads supported with TS-1 particles was observed via Scanning Electron Microscopy (SEM) (JEOL JSM 7401F, JEOL Ltd., Japan). Nitrogen adsorption–desorption isotherms were measured at 77 K on a Quantachrome Autosorb-1-C Chemisorption-Physisorption Analyzer. The specific surface area was calculated from the adsorption branches in the relative pressure range of 0.05–0.25. The mesopore diameter and mesopore size distribution were calculated from the desorption branches using the Barrett–Joyner–Halenda (BJH) method, whereas those for micropores were calculated by Saito–Foley (SF) method. The total pore volume was evaluated at a relative pressure of approximately 0.99. Transmission Electron Microscope (TEM) images were generated with a JEOL JEM-2011 high-resolution transmission electron microscope. Samples were characterized on a Bruker D8 Advanced

powder X-ray diffractometer (XRD) with $\text{CuK}\alpha$ radiation ($\lambda = 1.5418 \text{ \AA}$). The composite material was characterized by ultra-violet–visible (UV–vis) diffuse reflectance spectroscopy. The Ti element in the whole composite material was detected through Inductively Coupled Plasma atomic emission spectrometer (ICP, IRIS Intrepid II XSP from ThermoFisher Corp., America). Particle size was analyzed with a Mastersizer 2000 (Malvern Instruments Ltd., UK).

2.3. Oxidative desulfurization

DBT oxidation was performed in a 150 mL glass-stirred reactor equipped with a water-circulated condenser column. The reactor was immersed in a water bath to keep the reaction temperature at 343 K. A magnetic stirrer was used to blend the reaction mixture at a speed of 750 rpm. In a typical run, 1.0 g of the prepared catalyst and 35 g of the model fuel with DBT concentration of 150 ppm were added in the reactor and heated for 5 min. Approximately 0.08 mL of CHP (the molar ratio of CHP-to-DBT was 15) was then added into the reactor to start the reaction. Samples were taken after different reaction durations.

The reaction product was analyzed by gas chromatography (GC) 2014 with an FPD (SHIMADZU). The chromatographic column is Rat-Wax. The injector and the detector temperatures were both at 553 K. The oven temperature was maintained at 503 K for 5.3 min. Nitrogen gas with a flow rate of 30 mL/min was used as the carrier gas. The flow rate of hydrogen gas and air was 30 and 300 mL/min, respectively. DBT conversion was calculated with Eq. (1). The yield and space–time yield of DBT were defined as Eqs. (2) and (3), respectively,

$$X = \frac{\Delta n_{\text{DBT}}}{n_{\text{DBT}}} \quad (1)$$

$$\text{Yield} = \frac{n_{\text{DBTS}}}{n_{\text{DBT}}} \quad (2)$$

$$\text{STY} = \frac{g_{\text{DBTS}}}{g_{\text{TS-1}} \times t} \quad (3)$$

where Δn_{DBT} is the amount of DBT converted with the mole unit, n_{DBT} is the amount of DBT introduced with the mole unit, n_{DBTS} is the amount of the product, namely, dibenzothiophene sulfone (DBTS) with the mole unit after the reaction. g_{DBTS} and $g_{\text{TS-1}}$ are the mass amounts of DBTS and TS-1, respectively, and t is the reaction duration.

3. Results and discussion

3.1. Characteristics of porous glass beads supported with TS-1 particles

Surface morphologies of the porous glass supported with TS-1 nanoparticles are shown in Fig. 1(a) and (b). After TS-1 immobilization, the porous glass beads retained their spherical shape. The cross-section image of the as-prepared composite material is shown in Fig. 1(c), obviously, the surface of porous glass was almost covered by a monolayer of TS-1 particles with the thickness of less than 1 μm .

The surface morphology and pore size distribution of the porous glass beads treated with subcritical water are shown in Figs. 1 and 2 of the Supporting Material, respectively. The specific surface area of the porous glass beads reached 162.6 m^2/g . The pore volume and the mean pore diameter were 0.258 mL/g and 6.34 nm, respectively.

Pore size distributions of the mesopores and the isotherm of the as-prepared material are shown in Fig. 2(a) and (b), respectively. Fig. 2(c) shows the pore size distribution of the micropores. The

specific surface area, total pore volume, and mean pore diameter are listed in Table 1. The mean diameter and the pore volume of the micropores contained in the composite material were 0.45 nm and 0.150 mL/g , respectively.

Porous glass supported with TS-1 was examined by XRD (Fig. 3). The support, namely, porous glass, is amorphous, as confirmed by the absence of characteristic peaks. Meanwhile, porous glass loaded with TS-1 shows typical diffraction peaks at around 7.9°, 8.8°, 23.1°, and 23.9°, indexed to {011}, {020}, {051}, and {511}, respectively. These findings are excellent reflections of the MFI structure, indicating in-situ growth of TS-1 crystals on the porous glass beads successfully. The peak contributed by the {011} plane is a good evidence of Ti incorporation in the framework [28–32].

A TEM image of supported TS-1 particles is shown in Fig. 4(a), and the electron diffraction spectrum is shown in Fig. 4(b). TS-1 particles supported on the porous glass beads have uniform particle size and high crystallization. The discontinuous facula confirmed that the as-prepared TS-1 particles are single crystals [Fig. 4(b)]. The lattice fringes with a width of 1.12 nm are clearly observed in Fig. 4(c), which can be contributed to the {011} planes of TS-1 particles.

Porous glass beads with different Ti contents have been prepared by varying the mass ratio of the synthetic gel and porous glass beads. The amount of Ti in the whole material ranged from 0.285 to 0.507 wt.% determined by ICP. Therefore, combined with the results of XRD and TEM, it is confirmed the successful insertion of Ti element into the composite. The coordination state of the Ti species with great influence on the catalytic activity was investigated by UV–vis spectroscopy (Fig. 5). The sharp peak centered at 220 nm is ascribed to the tetrahedrally coordinated Ti^{4+} species incorporated in the framework [33–36]. No peaks were found around 240 or 330 nm, which are attributed to penta-coordinated Ti or small TiO_2 clusters through the quantum size effect [33,37]. Therefore, the Ti species in the composite material is tetrahedrally coordinated (Fig. 5).

3.2. Effect of reaction time and catalyst amount

Effects of reaction time and catalyst amount were investigated as shown in Fig. 6. The yield and conversion are equal in value because of the absence of any by-product during the experiment runs. The conversion increased steadily with the increase in reaction time until complete conversion of DBT. Compared with the reaction time, the catalyst amount has a more important role. The conversion was remarkably promoted by increasing the Ti content in catalyst. When the Ti amount increased from 0.285 to 0.414 wt.%, an abrupt increase in the conversion from 23.9% to 92.3% was observed within 5 min. For the catalyst with 0.507 wt.% of Ti, 85.7% of the feed has been converted just in 1 min, and the complete yield was obtained within 3 min.

ODS of DBT has been conducted in other studies [23,25,26] using TS-1 particles as the catalyst. Comparisons in catalytic performances in these studies are listed in Table 2. The space–time yield has been increased by one order of magnitude without any addition of solvent (e.g., alcohol, which is usually used in references) or metal nanoparticles.

Wang [28] has proven in his experiments that only the tetrahedrally coordinated Ti species is the active center for ODS, whereas that in the form of anatase shows much lower catalytic activity. Meanwhile, Kong et al. [14] reported that organosulfur compounds would be adsorbed by TS-1. Approximately 25% of thiophene was adsorbed by TS-1 after 240 min. In addition, we showed in our previous work [38] that organosulfur compounds would be physically adsorbed on the surface of porous glass beads by polar interactions. The capacities of the porous glass beads for benzothiophene (BT), DBT, and 4,6-DMDBT were 6.47 ± 0.09 , 8.58 ± 0.09 , and

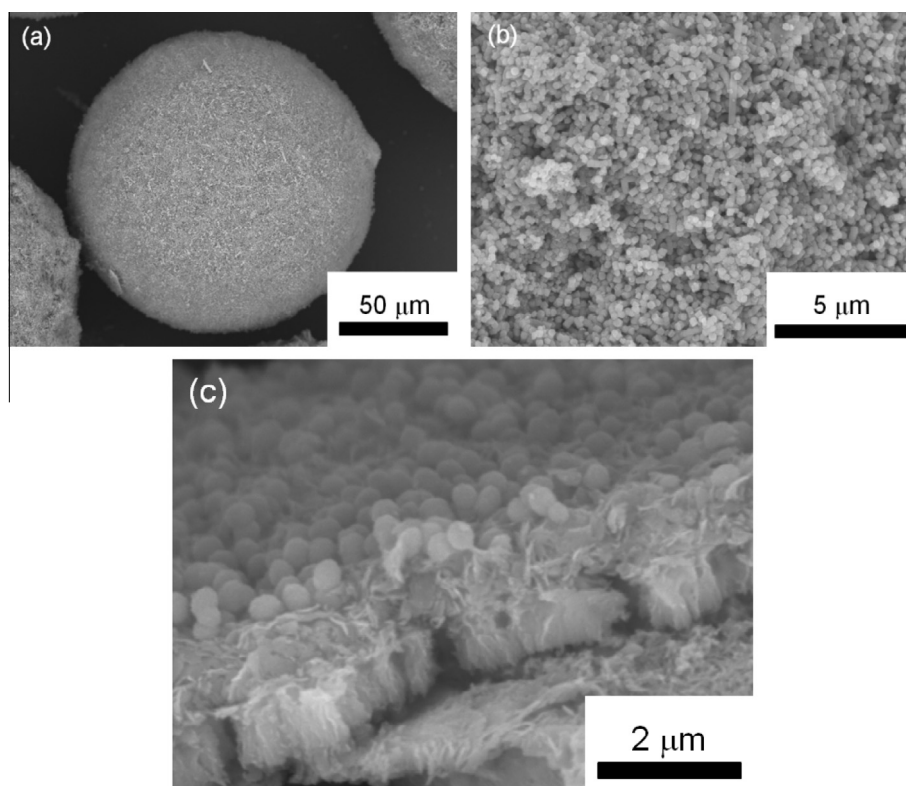


Fig. 1. (a and b) Surface morphologies of porous glass beads supported with TS-1; (c) cross-section image of porous glass beads supported with TS-1.

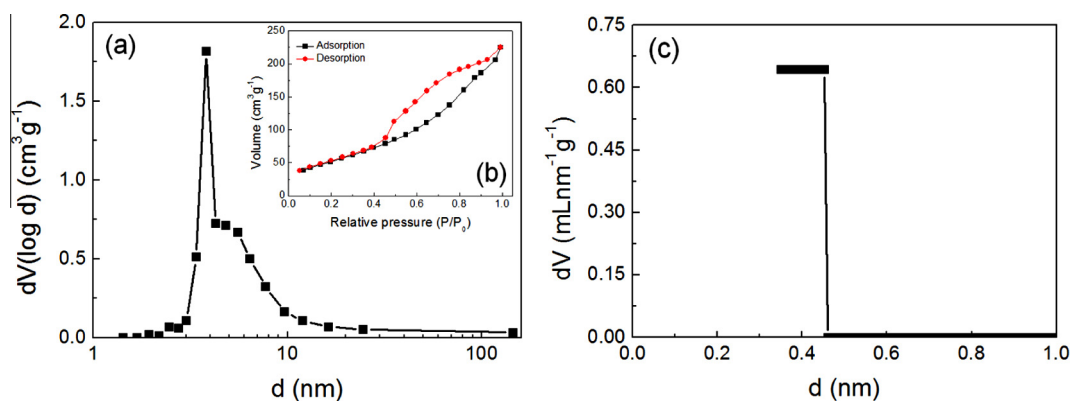


Fig. 2. (a) Mesopore size distribution of porous glass beads loaded with TS-1; (b) isotherm of the composite material; (c) micropore size distribution of the composite material.

Table 1

BET results of porous glass beads supported with TS-1.

Surface area (m^2/g)	Pore volume (mL/g)	Mean pore diameter (nm)
354.3	0.348	2.58

$11.20 \pm 0.08 \text{ mgS/g}_{\text{adsorbent}}$, respectively. The above references provided referable thoughts. Based on these results, we assume that the increase in the content of tetrahedrally coordinated Ti species is the main reason for the high catalytic performance through better adsorption for DBT.

Adsorptive experiment has been performed to verify the hypothesis. Three kinds of supported TS-1 with Ti content of 0.285, 0.366, and 0.507 wt.%, respectively were used as the adsorbent for DBT without addition of CHP [Fig. 7(a)]. After 20 min, TS-1

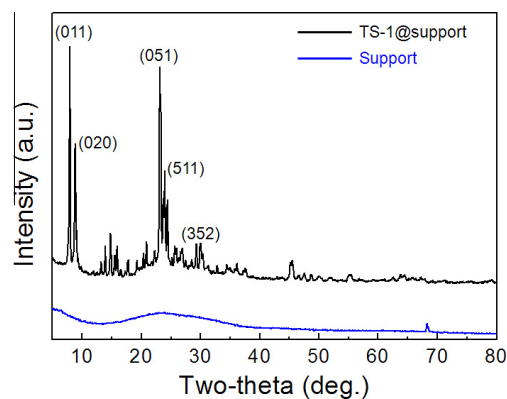


Fig. 3. XRD pattern of the TS-1-decorated porous glass beads.

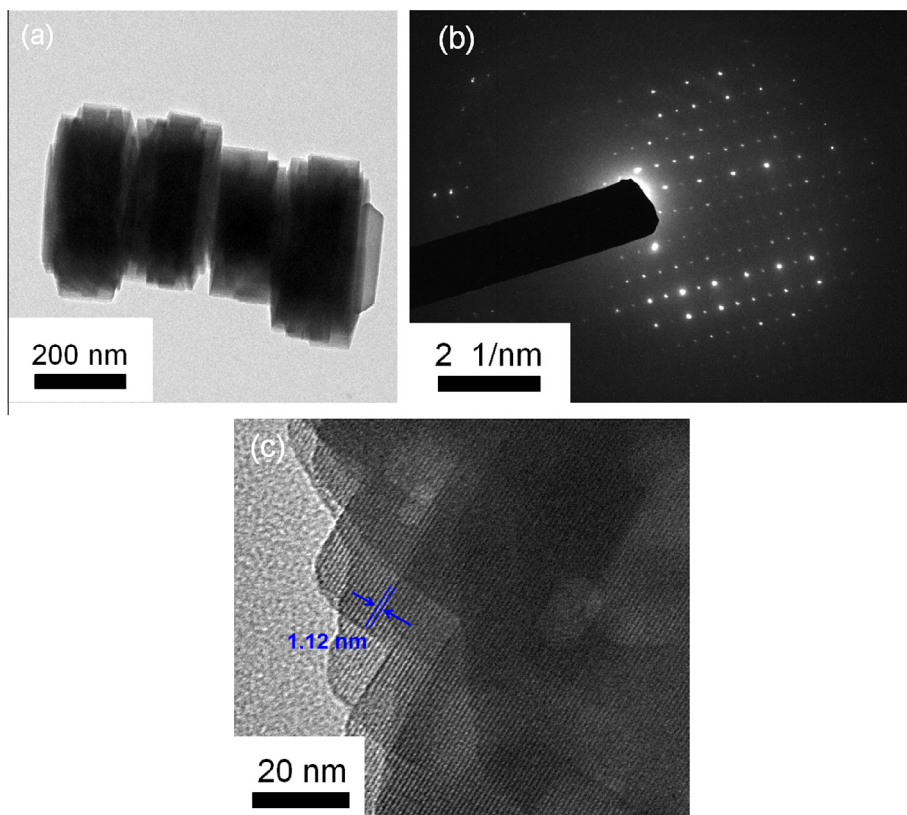


Fig. 4. (a and c) TEM images of TS-1 particles; (b) electron diffraction spectrum of TS-1 particles.

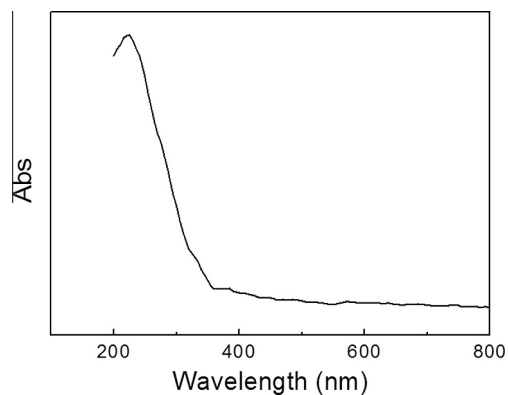


Fig. 5. UV-vis diffuse reflectance spectra of porous glass beads supported with TS-1.

with the largest Ti content showed the highest removal rate of 1.51% for DBT, whereas that with 0.285 wt.% Ti provided the lowest removal rate of only 0.40%. The experimental result confirmed our hypothesis.

Computer simulation is a powerful tool for exploring the interactions between molecules. Thus, Materials Studio, a work station developed by Accelrys Software Inc., was used to provide insight into the interaction between the TS-1 particles and the DBT molecule, which involves three main steps. First, a surface of TS-1 crystal is built and optimized. Second, DBT is added onto the surface built in the first step. Third, molecular dynamics is simulated, and then the energy is calculated. Material Visualizer, Amorphous Cell, and Discover were used in the third step. The smart minimizer method was used during the energy minimization process, and the force field was compass during the energy calculation. Interaction

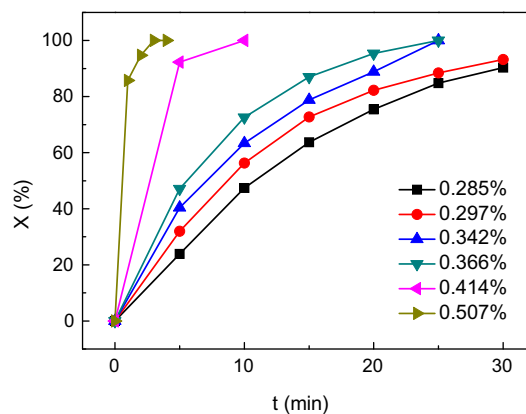


Fig. 6. Effects of reaction time and catalyst amount on conversion. Initial concentration of DBT: 150 ppm, reaction temperature: 343 K; O/S: 15.

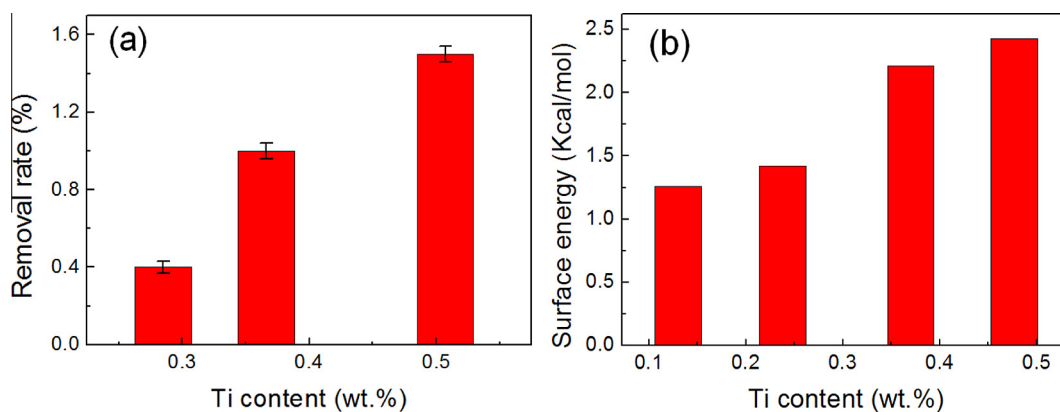
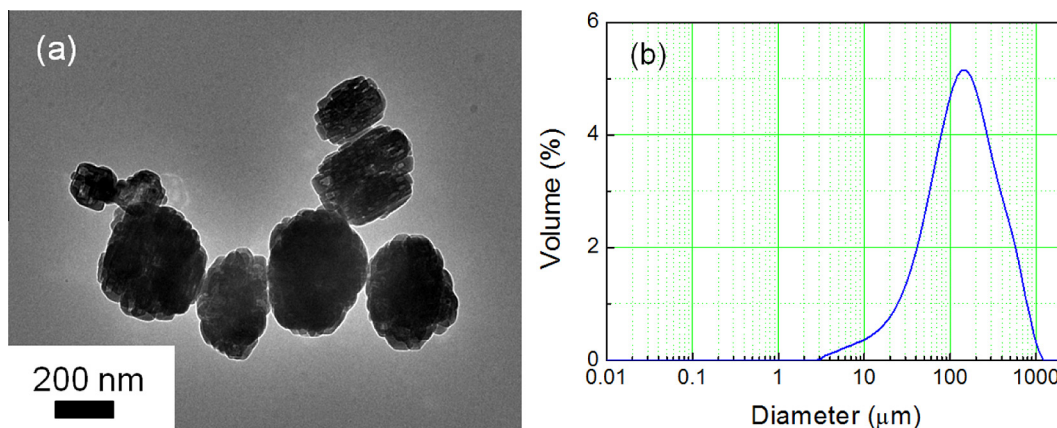
between the surface of TS-1 and the DBT was calculated as $E_{\text{interaction}} = E_{\text{total}} - (E_{\text{surface}} + E_{\text{DBT}})$. The simulation result is shown in Fig. 7(b). TS-1 with Ti contents of 0.131, 0.238, 0.370, and 0.477 wt.% were simulated, and the corresponding surface energies between them and the DBT molecule ranged in the same order. Larger surface energy results in stronger interaction between the TS-1 particles and DBT. The adsorption of the reactant is the first step in a solid catalyst fluid phase heterogeneous reaction, such that enhanced adsorption property of the reactant onto the surface of the catalysts helps enhance the reaction.

In a nutshell, both the experimental result and the computer simulation are consistent with the hypothesis that the tetrahedrally coordinated state of Ti species in the as-prepared TS-1 supported on porous glass beads contributed to high catalytic activity.

Table 2

Comparisons in catalytic performance with other works (selectivity is 100% in all the works).

Reaction duration (min)	Reaction temperature (K)	Catalyst amount (g)	X (%)	STY ($\text{g}_{\text{DBT}}/(\text{g}_{\text{TS-1}} \text{ min})$)	References
3	343	0.015	100	0.14	This work
180	323	/	6	/	[23]
180	323	0.050	90	9.00×10^{-3}	[25]
180	353	0.120	95	0.50×10^{-3}	[26]

**Fig. 7.** (a) Adsorption of DBT onto immobilized TS-1 with different Ti content; (b) surface energy between TS-1 and DBT.**Fig. 8.** (a) TEM images of commercial TS-1 particles; (b) particle size distribution of commercial TS-1: $d(0.1) = 32.569 \mu\text{m}$; $d(0.5) = 129.978 \mu\text{m}$; $d(0.9) = 425.120 \mu\text{m}$.

In addition to the coordinated state of Ti, the actual particle size explored to the reactant during the reaction is considered as the other major influencing factor. Fixed on the surface of porous glass beads, TS-1 particles in our work maintained their original nano version, and this was verified by the SEM and TEM images. The crystalline size of the commercial TS-1 particles was determined by TEM [Fig. 8(a)]. The particle size distribution in the reaction system was characterized with a particle size analyzer [Fig. 8(b)]. Nanosized TS-1 crystals tend to agglomerate in the reaction system with the $d(0.9)$ of 425 μm . The surface area which was explored to the reactant during the reaction is sharply reduced because of the agglomeration. And in order to prove the point stated above, the catalytic performance of TS-1 particles prepared in this work has also been investigated. As expected, only 6% conversion of DBT was obtained after 5 min which was much lower than that of immobilized TS-1 particles. Similar result has also been reported by Yeung and coworkers [32]. In their work, a monolayer of TS-1 nanocrystals was uniformly deposited on the SiO_2 beads surface

and the thin shell catalyst exhibited both high turnover number and good selectivity compared to powder catalysts.

3.3. Effects of initial concentration, amount of oxidant, and temperature on conversion

The catalytic performance of supported TS-1 under various initial sulfur concentrations are presented in Fig. 9(a). Longer reaction duration is needed for complete conversion of DBT by increasing the initial concentration of DBT. 100% conversion was obtained in just 2 min with the initial concentration of 70 ppm. When the initial concentration turned to 2000 ppm, 94% of DBT was converted after 30 min.

The effect of oxidant amount was determined in relation to the changes in DBT conversion [Fig. 9(b)]. With the increase in the mole ratio of CHP-to-DBT, the reaction rate first increased and then decreased. When the ratio of CHP-to-DBT was smaller than 10, the reaction rate was greatly promoted by the addition of more CHP as

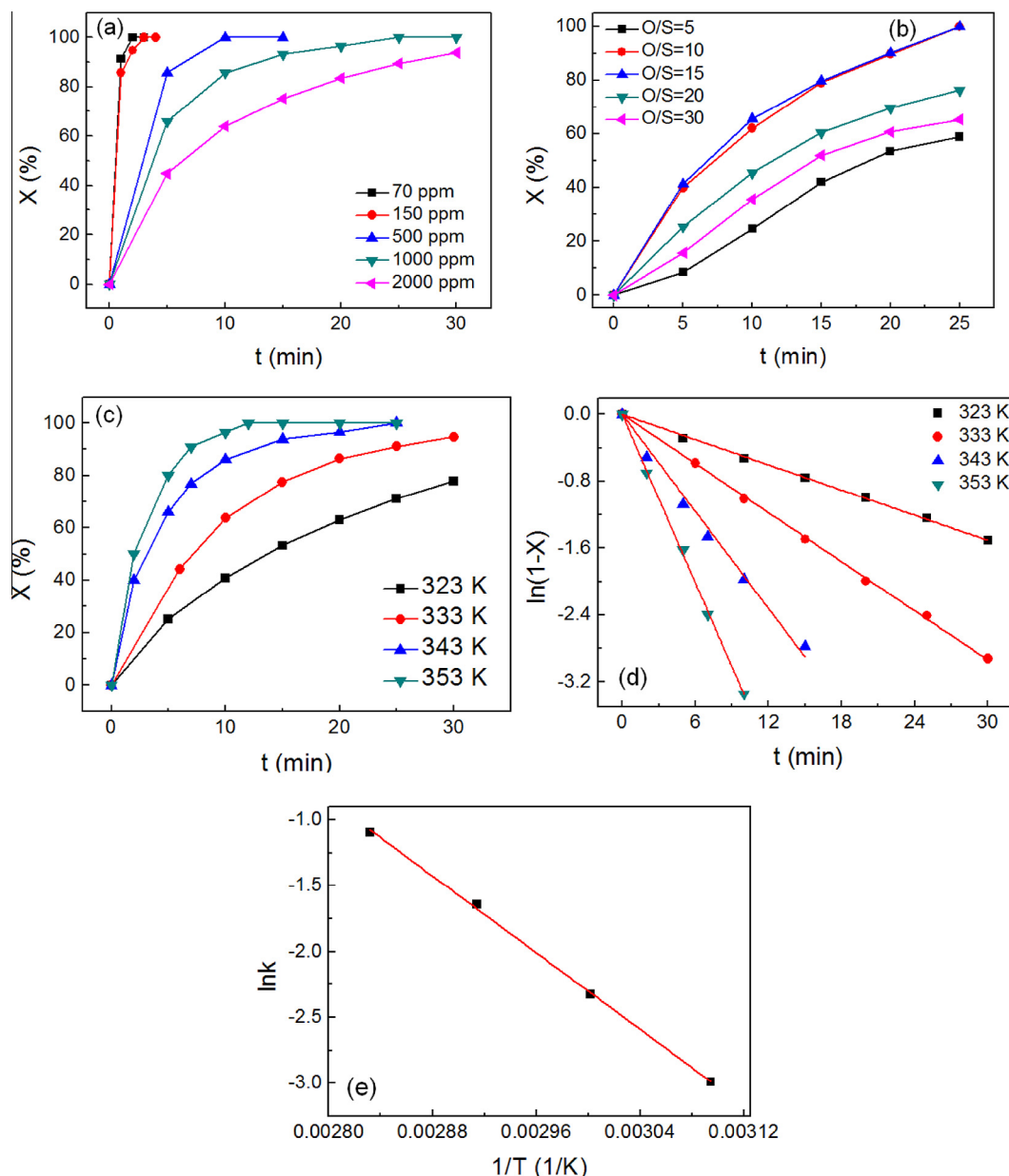


Fig. 9. (a) Effect of initial concentration of DBT on conversion; (b) effect of amount of oxidant on conversion; (c) effect of temperature on conversion; (d) fitting of experimental data to the pseudo-first-order rate model; (e) Arrhenius plot.

a result of more hydroxyl radicals produced. However, when further increase in CHP was realized, the oxidation of DBT was hindered by consumption of hydroxyl radicals [39].

The effect of reaction temperature was investigated, and the results are shown in Fig. 9(c). The reaction rate was promoted at higher temperatures. The conversion increased from 25.1% to 80.2% when the temperature varied from 323 to 353 K, with fixed reaction duration of 5 min.

The oxidative reaction of sulfur-containing compound is considered as a pseudo-first-order reaction, where the rate is apparently dependent on the concentration of the limiting reactant [23,25,40]. The reaction rate can be described by Eq. (4):

$$-r_A = -\frac{dC_A}{dt} = kC_A \quad (4)$$

where k is the apparent rate constant, and A is the limiting reactant (DBT).

After the integration of Eq. (4), the relationship between X and reaction time can be obtained by Eq. (5):

$$\ln(1 - X) = -kt \quad (5)$$

The value of $\ln(1 - X)$, which was calculated from the data, is plotted as a function of reaction time (t) at 323, 333, 343, and 353 K, respectively [Fig. 9(d)]. The straight lines at different temperatures are fitted with good correlation coefficients, verifying that the kinetic obeys the pseudo-first-order. The rate constant was calculated to be 0.0503, 0.0980, 0.1936, and 0.3353 min^{-1} , respectively. The corresponding R^2 values are 0.9995, 0.9998, 0.9956, and 0.9996, respectively.

Based on the Arrhenius equation, the activation energy (E) can be calculated using Eq. (6):

$$\ln k = \ln k_0 - \frac{E}{RT} \quad (6)$$

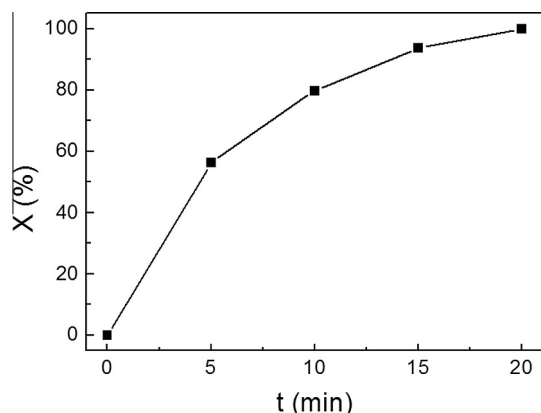


Fig. 10. Oxidation of 4,6-DMDBT; initial concentration of 4,6-DMDBT: 500 ppm, reaction temperature: 343 K; O/S: 15.

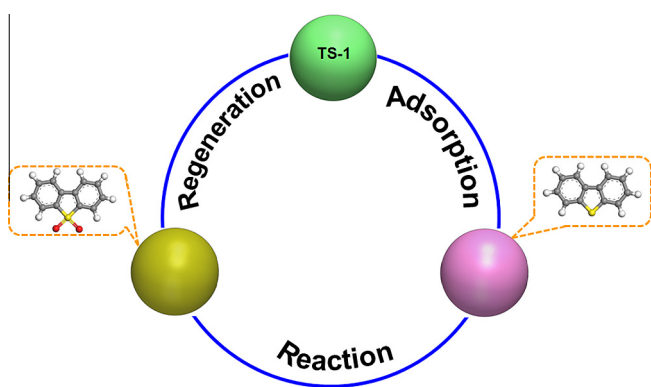


Fig. 11. Transformation of TS-1 catalyst during the reaction.

where k_0 is the frequency factor or pre-exponential factor (min^{-1}).

The plot of $\ln k$ versus $1/T$ is shown in Fig. 9(e), giving a linear plot with the R^2 of 0.9989. The activation energy was calculated to be 60.5 kJ/mol.

3.4. Oxidation of 4,6-DMDBT

The methylated derivatives of DBT are considered to be the most refractory compounds in HDS. In this work, the oxidation of 4,6-DMDBT was investigated as well. Fig. 10 illustrates that 4,6-DMDBT could also be effectively oxidized but the reaction rate was lower because of the steric hindrance. 56.3% of 4,6-DMDBT was converted in 5 min and complete conversion was obtained in 20 min.

3.5. Regeneration performance

The reaction rate slowed down as the reaction processed, and the catalyst turned yellow after the reaction, which may be caused by the adsorption of DBTs. Fig. 11 shows that the DBT molecules were first physically adsorbed on the surface of TS-1, and then reacted with the oxidant, transforming to DBTS. The sulfur content of the used catalyst is 0.091 wt.% as characterized by ICP, thereby verifying the speculation. Desulfurization catalyst must be regenerated for multiple cycles. Therefore, regeneration of the spent catalyst is necessary. Based on our previous study [38], thermal treatment is highly efficient in the removal of adsorbed organosulfur compounds.

The results of the regeneration test are shown in Fig. 12(a). The used catalyst was calcinated for 4 h at 823 K. Compared with the fresh catalyst, the conversion did not decrease even after three cycles. SEM images and UV–vis diffuse reflectance spectra of the catalyst after three cycles are shown in Fig. 12(b) and (c), respectively. TS-1 particles are still homogeneously dispersed on the surface of porous glass beads. The sharp peak centered at 220 nm

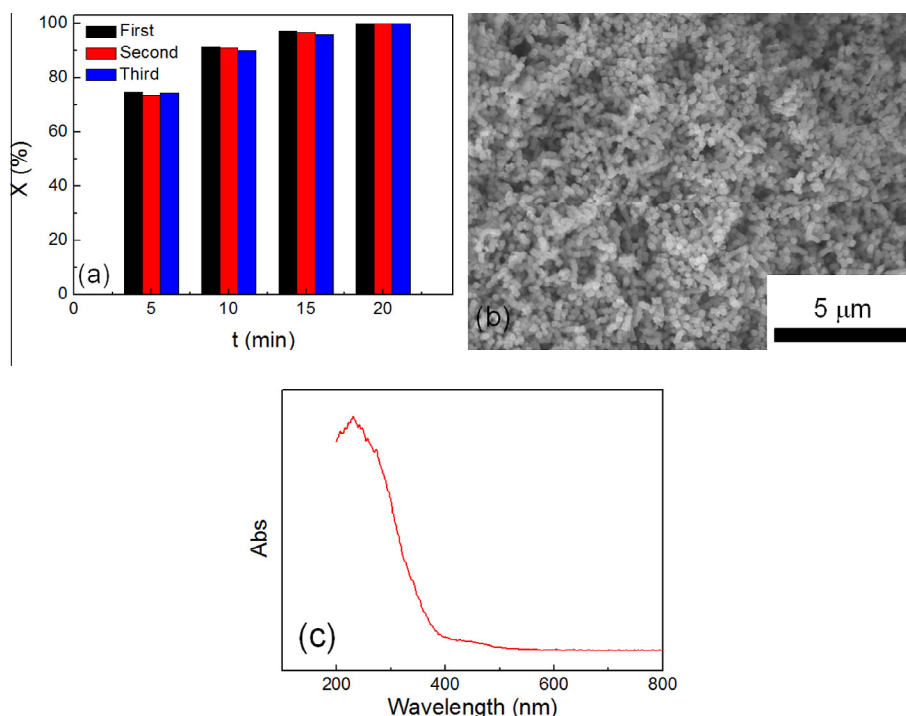


Fig. 12. (a) Stability test of the catalyst. Ti content: 0.507 wt.%; reaction temperature: 343 K; O/S: 15; (b) SEM images of catalyst after three circles; (c) UV–vis diffuse reflectance spectra of catalyst after three circles.

was still observed and no peaks were found around 240 nm or 330 nm, indicating the existence of tetrahedrally coordinated Ti^{4+} species in the framework. The Ti content after the three reaction cycles was determined by ICP to be 0.506 wt.%, strongly supporting the catalytic activity result. The physical characterization and the regeneration result agreed with each other and verified the good stability of the as-prepared catalyst. The ease of regeneration of the catalyst indicates that the porous glass beads supported with TS-1 are suitable and feasible in practical applications.

4. Conclusion

Egg-shell structured TS-1/porous glass materials were successfully prepared and used as the catalyst for ODS. Uniform-sized TS-1 particles were homogeneously dispersed on the surface of the porous glass beads. The prepared catalyst showed excellent performance for DBT oxidation. Several affecting factors were investigated. The amount of oxygen radical anion increased with the increase in mole ratio of O/S from 5 to 15, resulting in the hastening of the reaction rate. However, with further increase in O/S, the probability of two oxygen radical anions combining to oxygen molecule was much higher, leading to a negative influence on the reaction. The reaction was promoted by increasing the catalyst content or the reaction temperature. Complete conversion was reached by the catalyst with Ti content of 0.507 wt.% at 343 K within 3 min, and 100% recovery in catalytic activity after 3 cycles was demonstrated. DBT oxidation is a pseudo first-order reaction with the activation energy of 60.5 kJ/mol. Compared with other studies, the space–time yield has been increased by one order of magnitude without any addition of solvent (e.g., alcohol, which is usually used in references) or metal nanoparticles. The coordinated state of Ti species has an important role in the catalytic activity which has been verified both by experimental result and computer simulation. The immobilization of TS-1 nanoparticles helps to explore larger surface area, which is the other major reason for the high activity. To deeply understand the catalytic mechanism, further studies would be conducted such as the kinetic and the search for the transition states.

Acknowledgements

We gratefully acknowledge the support of the National Basic Research Foundation of China (Grant No. 2013CB733600) and the National Natural Science Foundation of China (21036002, 91334201, 21276140).

Appendix A. Supplementary data

Supplementary data associated with this article can be found, in the online version, at <http://dx.doi.org/10.1016/j.cej.2014.08.027>.

References

- [1] U.S.EPA, January 2001.
- [2] U.S.EPA, April 2001.
- [3] C.N. Satterfield, in: J.C. James, R.F. James, S.P. Max, R.S. William, W. James (Eds.), *Heterogeneous Catalysis in Industrial Practice*, second ed., McGraw-Hill, New York, 1991, p. 378.
- [4] J.G. Speight, in: H. Heinz, *The Chemistry and Technology of Petroleum*, third ed., Marcel Dekker, New York, 1998.
- [5] I.V. Babich, J.A. Moulijn, *Science and technology of novel processes for deep desulfurization of oil refinery streams: a review*, *Fuel* 82 (2003) 607–631.
- [6] A.J. Hernandez-Maldonado, F.H. Yang, G.S. Qi, R.T. Yang, *Desulfurization of transportation fuels by pi-complexation sorbents: Cu(I)-, Ni(II)-, and Zn(II)-zeolites*, *Appl. Catal. B* 56 (2005) 111–126.
- [7] F. Zannikos, E. Lois, S. Stournas, *Desulfurization of petroleum fractions by oxidation and solvent-extraction*, *Fuel Process Technol.* 42 (1995) 35–45.
- [8] S. Otsuki, T. Nonaka, N. Takashima, W.H. Qian, A. Ishihara, T. Imai, T. Kabe, *Oxidative desulfurization of light gas oil and vacuum gas oil by oxidation and solvent extraction*, *Energy Fuels* 14 (2000) 1232–1239.
- [9] J.M. Campos-Martin, M.C. Capel-Sanchez, P. Perez-Presas, J.L.G. Fierro, *Oxidative processes of desulfurization of liquid fuels*, *J. Chem. Technol. Biotechnol.* 85 (2010) 879–890.
- [10] Z. Ismagilov, S. Yashnik, M. Kerzhentsev, V. Parmon, A. Bourane, F.M. Al-Shahrani, A.A. Hajji, O.R. Koseoglu, *Oxidative desulfurization of hydrocarbon fuels*, *Catal. Rev. Sci. Eng.* 53 (2011) 199–255.
- [11] S.Q. Ma, G. Li, X.S. Wang, *The direct synthesis of hydrogen peroxide from H_2 and O_2 over Au/TS-1 and application in oxidation of thiophene in situ*, *Chem. Lett.* 35 (2006) 428–429.
- [12] D.J. Robinson, L. Davies, N. McGuire, D.F. Lee, P. McMorn, D.J. Willock, G.W. Watson, P.C.B. Page, D. Bethell, G.J. Hutchings, *Oxidation of thioethers and sulfoxides with hydrogen peroxide using TS-1 as catalyst*, *Phys. Chem. Chem. Phys.* 2 (2000) 1523–1529.
- [13] L.Y. Kong, G. Li, X.S. Wang, *Kinetics and mechanism of liquid-phase oxidation of thiophene over TS-1 using H_2O_2 under mild conditions*, *Catal. Lett.* 92 (2004) 163–167.
- [14] L.Y. Kong, G. Li, X.S. Wang, B. Wu, *Oxidative desulfurization of organic sulfur in gasoline over Ag/TS-1*, *Energy Fuels* 20 (2006) 896–902.
- [15] L.Y. Kong, G. Li, X.S. Wang, *Mild oxidation of thiophene over TS-1/ H_2O_2* , *Catal. Today* 93–95 (2004) 341–345.
- [16] S. Cui, F. Ma, Y. Wang, *Oxidative desulfurization of model diesel oil over Ti-containing molecular sieves using hydrogen peroxide*, *React. Kinet. Catal. Lett.* 92 (2007) 155–163.
- [17] C. Jin, G. Li, X. Wang, Y. Wang, L. Zhao, D. Sun, *A titanium containing micro/mesoporous composite and its catalytic performance in oxidative desulfurization*, *Micropor. Mesopor. Mater.* 111 (2008) 236–242.
- [18] D. Huang, Y.J. Wang, Y.C. Cui, G.S. Luo, *Direct synthesis of mesoporous TiO_2 and its catalytic performance in DBT oxidative desulfurization*, *Micropor. Mesopor. Mater.* 116 (2008) 378–385.
- [19] Y. Jia, G. Li, G. Ning, C. Jin, *The effect of N-containing compounds on oxidative desulfurization of liquid fuel*, *Catal. Today* 140 (2009) 192–196.
- [20] A.T. Shah, B. Li, Z.E.A. Abdalla, *Direct synthesis of Ti-containing SBA-16-type mesoporous material by the evaporation-induced self-assembly method and its catalytic performance for oxidative desulfurization*, *J. Coll. Interf. Sci.* 336 (2009) 707–711.
- [21] T. Napanang, T. Sooknoi, *Oxidative extraction of thiophene from n-dodecane over TS-1 in continuous process: a model for non-severe sulfur removal from liquid fuels*, *Catal. Commun.* 11 (2009) 1–6.
- [22] C. Shi, B. Zhu, M. Lin, J. Long, *Synthesis and characterization of NTS material and its oxidation desulfurization properties*, *Catal. Today* 149 (2010) 132–137.
- [23] N. Jose, S. Sengupta, J.K. Basu, *Optimization of oxidative desulfurization of thiophene using Cu/titanium silicate-1 by box-behnken design*, *Fuel* 90 (2011) 626–632.
- [24] X. Wang, G. Li, W. Wang, C. Jin, Y. Chen, *Synthesis, characterization and catalytic performance of hierarchical TS-1 with carbon template from sucrose carbonization*, *Micropor. Mesopor. Mater.* 142 (2011) 494–502.
- [25] A. Sengupta, P.D. Kamble, J.K. Basu, S. Sengupta, *Kinetic study and optimization of oxidative desulfurization of benzothiophene using mesoporous titanium silicate-1 catalyst*, *Ind. Eng. Chem. Res.* 51 (2012) 147–157.
- [26] Y. Seung-Tae, J. Kwang-Eun, J. Soon-Yong, A. Wha-Seung, *Synthesis of mesoporous TS-1 using a hybrid SiO_2 - TiO_2 xerogel for catalytic oxidative desulfurization*, *Mater. Res. Bull.* 47 (2012) 4398–4402.
- [27] Y. Zhu, Z. Hua, X. Zhou, Y. Song, Y. Gong, J. Zhou, J. Zhao, J. Shi, *CTAB-templated mesoporous TS-1 zeolites as active catalysts in a desulfurization process: the decreased hydrophobicity is more favourable in thiophene oxidation*, *RSC Adv.* 3 (2013) 4193–4198.
- [28] W. Wang, G. Li, L. Liu, Y. Chen, *Synthesis and catalytic performance of hierarchical TS-1 directly using agricultural products sucrose as meso/macropores template*, *Micropor. Mesopor. Mater.* 179 (2013) 165–171.
- [29] A. Thangaraj, R. Kumar, S.P. Mirajkar, P. Ratnasamy, *Catalytic properties of crystalline titanium silicalites. 1. Synthesis and characterization of titanium-rich zeolites with MFI structure*, *J. Catal.* 130 (1991) 1–8.
- [30] L.T.Y. Au, J.L.H. Chau, C.T. Ariso, K.L. Yeung, *Preparation of supported SiI-1, TS-1 and VS-1 membranes – effects of Ti and V metal ions on the membrane synthesis and permeation properties*, *J. Membr. Sci.* 183 (2001) 269–291.
- [31] Q. Zhao, P. Li, D. Li, X. Zhou, W. Yuan, X. Hu, *Synthesis and characterization of titanium silicate-1 supported on carbon nanofiber*, *Micropor. Mesopor. Mater.* 108 (2008) 311–317.
- [32] X. Wang, X. Zhang, Y. Wang, H. Liu, J. Wang, J. Qiu, H.L. Ho, W. Han, K.L. Yeung, *Preparation and performance of TS-1/ SiO_2 egg-shell catalysts*, *Chem. Eng. J.* 175 (2011) 408–416.
- [33] F. Geobaldo, S. Bordiga, A. Zecchina, E. Giamello, G. Leofanti, G. Petrini, *DRS UV-vis and EPR spectroscopy of hydroperoxo and superoxo complexes in titanium silicalite*, *Catal. Lett.* 16 (1992) 109–115.
- [34] T. Blasco, M.A. Camblor, A. Corma, J. Perezpariente, *The state of Ti in titanoaluminosilicates isomorphous with zeolite-beta*, *J. Am. Chem. Soc.* 115 (1993) 1180613.

- [35] E. Jorda, A. Tuel, R. Teissier, J. Kervennal, TiF₄: an original and very interesting precursor to the synthesis of titanium containing silicalite-1, *Zeolites* 19 (1997) 238–245.
- [36] C. Perego, A. Carati, P. Ingallina, M.A. Mantegazza, G. Bellussi, Production of titanium containing molecular sieves, and their application in catalysis, *Appl. Catal. A* 221 (2001) 63–72.
- [37] G. Deo, A.M. Turek, I.E. Wachs, D.R.C. Huybrechts, P.A. Jacobs, Characterization of titania silicalites, *Zeolites* 13 (1993) 365–373.
- [38] C. Shen, Y.J. Wang, J.H. Xu, Y.C. Lu, G.S. Luo, Porous glass beads as a new adsorbent to remove sulfur-containing compounds, *Green Chem.* 4 (2012) 1009–1015.
- [39] D. Zhao, J. Zhang, J. Wang, W. Liang, H. Li, Photocatalytic oxidation desulfurization of diesel oil using Ti-containing zeolite, *Pet. Sci. Technol.* 27 (2009) 1–11.
- [40] M. Te, C. Fairbridge, Z. Ring, Oxidation reactivities of dibenzothiophenes in polyoxometalate/H₂O₂ and formic acid/H₂O₂ systems, *Appl. Catal. A* 219 (2001) 267–280.